Low-Energy Λ-Proton Elastic Scattering*

B. SECHI-ZORN, B. KEHOE, AND J. TWITTY†
University of Maryland, College Park, Maryland 20742
AND
R. A. BURNSTEIN
Illinois Institute of Technology, Chicago, Illinois 60616
(Received 18 July 1968)

The cross sections for Λ-p elastic scattering with Λ momenta in the interval 110–330 MeV/c have been measured. Our results are based on 224 scattering events found in a sample of 95 600 Λ hyperons observed in an exposure of the 81-cm Saclay hydrogen bubble chamber to a stopping K^- beam. These cross sections are analyzed in terms of effective-range theory. A wide spectrum of solutions in this formalism give acceptable agreement with the data.

I. INTRODUCTION

UNTIL recently, experimental information on Λ-proton interactions has come primarily from measurements of hyperfragment binding energies.[1–3] During the last few years, this information has been supplemented by direct measurement of Λ-proton elastic scattering in bubble chambers.[4,5] This paper reports on a measurement of the differential and total elastic cross section for Λ-p scattering at low momenta.[6]

In Sec. II the experimental method is described, in Sec. III the cross sections are presented and compared with other data, and in Sec. IV these results are analyzed in terms of the effective-range formalism and related to theoretical models and the results of hyperfragment analysis.

II. SCANNING AND MEASURING

This experiment is based upon an exposure of the Saclay 81-cm hydrogen bubble chamber[7] to a separated K^- beam[8] at the CERN proton synchrotron. The particles were transported at 800 MeV/c and slowed down by a 20-cm copper absorber so that the K^- mesons entered the chamber with a momentum of about 230 MeV/c. In each photograph, an average of about three K^- mesons came to rest in the visible portion of the chamber.

This study is based upon 100 000 pictures in which 95 627 Λ hyperons were observed. The Λ hyperons were produced from the following direct K^- interactions:

$$K^- + p \to \Lambda + \pi^0, \quad (1)$$

$$K^- + p \to \Sigma^0 + \pi^0, \quad \Sigma^0 \to \Lambda + \gamma, \quad (2)$$

and from the Σ^- interactions:

$$\Sigma^- + p \to \Lambda + n, \quad (3)$$

$$\Sigma^- + p \to \Sigma^0 + n, \quad \Sigma^0 \to \Lambda + \gamma, \quad (4)$$

where the Σ^- are produced in the reaction

$$K^- + p \to \Sigma^- + \pi^+. \quad (5)$$

Figure 1 shows the Λ momentum spectrum from K^--p interactions at rest. Reaction (2) yields a Λ spectrum from about 90 to 250 MeV/c and is the primary source of Λ's ($\sim$70%).[9] There are two additional and approximately equal contributions[9] to the Λ spectrum: Reaction (1) gives rise to Λ's with momentum 254 MeV/c, and reactions (3) and (4) give rise to Λ's with momentum 290 MeV/c and a spectrum from 0 to 130 MeV/c, respectively. In addition to these sources of Λ hyperons, there is a small source ($\sim$10%), not shown in Fig. 1, from in-flight K^--p and Σ^--p interactions. These processes give rise to a Λ spectrum extending from 0 to 360 MeV/c.

The film scanning was done on pairs of Recordak[10] projectors using two of the three available views. The procedure involved an "area scan" on both views for

* Work supported at the University of Maryland by the U. S. Atomic Energy Commission under Contract No. AEC-ORO-2504-123 and at the Illinois Institute of Technology in part by the National Science Foundation under Grant No. GP-7404.

† Present address: University of Wisconsin, Madison, Wis.

[1] For review articles on measurements of hyperfragment binding energies, see R. G. Ammar, CERN Report No. 64-1, 1963, p. 7 (unpublished); R. Levi-Setti, *ibid.*, p. 17.

[2] R. H. Dalitz and B. W. Downs, Phys. Rev. **111**, 967 (1958); B. W. Downs and R. H. Dalitz, Phys. Rev. **114**, 593 (1959); B. W. Downs, CERN Report No. 64-1, 1963, p. 173 (unpublished).

[3] R. H. Dalitz, in Conference on the Use of Elementary Particles in Nuclear Structure Research, University of Brussels, 1965 (unpublished), and references contained therein.

[4] B. Sechi-Zorn, R. A. Burnstein, T. B. Day, B. Kehoe, and G. A. Snow, Phys. Rev. Letters **13**, 282 (1964); G. Alexander, U. Karshon, A. Shapira, G. Yekutieli, R. Engelmann, H. Filthuth, A. Fridman, and A. Minguzzi-Ranzi, *ibid.* **13**, 484 (1964).

[5] G. Alexander, O. Benary, U. Karshon, A. Shapira, G. Yekutieli, R. Engelmann, H. Filthuth, A. Fridman, and B. Schiby, Phys. Rev. Letters **19**, 715 (1966); *Proceedings of the International Conference on High-Energy Physics and Nuclear Structure at Rehovoth, Israel* (North-Holland Publishing Company, Amsterdam 1967).

[6] Preliminary accounts of this experiment appeared in Phys. Rev. Letters **13**, 282 (1964) and in University of Maryland Technical Report No. 469, 1965 (unpublished).

[7] P. Baillon, thesis, University of Paris, 1963 (unpublished).

[8] A description of the beam is given by B. Aubert, H. Courant, H. Filthuth, A. Segar, and W. Willis, in *Proceedings of the International Conference on Instrumentation for High-Energy Physics at CERN* (North-Holland Publishing Company, Amsterdam, 1963).

[9] These proportions are derived from the Humphrey-Ross ratios [W. H. Humphrey and R. R. Ross, Phys. Rev. **127**, 1305 (1962)], and our result that 12.5±1% of the initial Σ^- hyperons interact at rest.

[10] Trademark, Eastman Kodak Company, Inc.

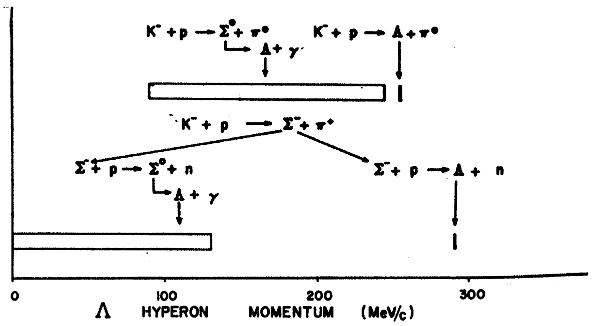

FIG. 1. Momentum spectrum of Λ hyperons resulting from K^--p interactions at rest.

charged Λ decays. It consisted of first scanning by area for Λ-particle decay products and then searching for possible origins for the Λ's found. The origins were of two types: (A) the vertices of the reactions (1) to (4) previously mentioned, or (B) proton recoils from the reaction $\Lambda+p \rightarrow \Lambda+p$. If an origin was of type A, a further search for a proton was made; if it was an origin of type B, an origin of type A for the incoming Λ was looked for. A Λ that could not be connected to any of the reactions (1) to (4) was looked at by a physicist and if no origin was found, the event was eliminated. As a consistency check, every K^- entering the bubble chamber was followed from its entry point to a K^--p interaction or decay vertex or to its exit from the chamber. If an interaction with the configuration associated with reactions (1) or (2) or with (5) followed by (3) or (4) was found, a further search for Λ decays and scatters was made. Every Λ found was recorded and rescanning of 30 000 pictures gave a scanning efficiency for Λ decays of 98%.

Events were measured on standard digitized film-plane measuring machines. The program PACKAG[11] was used for the geometrical reconstruction and kinematic fitting of the events. Two classes of events were measured. One class of events involved Λ decays without associated proton recoils, for use in the path-length determination, and the other class of events involved candidate Λ-p scattering events.

Figure 2 is a line drawing and photograph of a typical Λ-p scattering event. The kinematic fitting program tested the following hypotheses.

(1) Λ decay at point C from an origin at A;
(2) Λ decay at C from an origin at B;
(3) Λ origin at A and scatter at B [for the events satisfying hypothesis (2)].

In general, the fitting procedure yielded a sharp separation between truly scattered and unscattered Λ's.

[11] PACKAG is a combination of the programs PANG and KICK. For a description of the program KICK, see Reference Manual for KICK IBM Program, edited by A. H. Rosenfeld, University of California Radiation Laboratory Report No. 9099 (unpublished); and A. H. Rosenfeld and J. N. Snyder, Rev. Sci. Instr. **33**, 181 (1962). The University of Maryland version has been modified extensively by Professor T. B. Day and Professor R. G. Glasser.

III. CROSS-SECTION DETERMINATION

The 336 events which fit the Λ-p scattering hypothesis are displayed on Fig. 3(b). Each event is positioned according to the Λ center-of-mass scattering angle and the incident Λ laboratory momentum. The 336 events were subjected to a set of five geometric criteria which were applied to the events in order to insure a high and uniform detection efficiency.

These geometrical criteria were as follows:

(i) The point of origin of the Λ was required to be within a specified fiducial volume.

(ii) The projected length of the Λ, between production and scatter, was required to be greater than 0.5 mm.

(iii) The projected length of the recoil proton was required to be greater than 2.0 mm.

(iv) The projected length of the scattered Λ was required to to greater than 0.5 mm.

(v) The projected length of the proton from the Λ decay was required to be greater than 1.0 mm.

A weighting factor for each of the uncut events was obtained by means of a numerical integration which took into account all the above geometric criteria. An

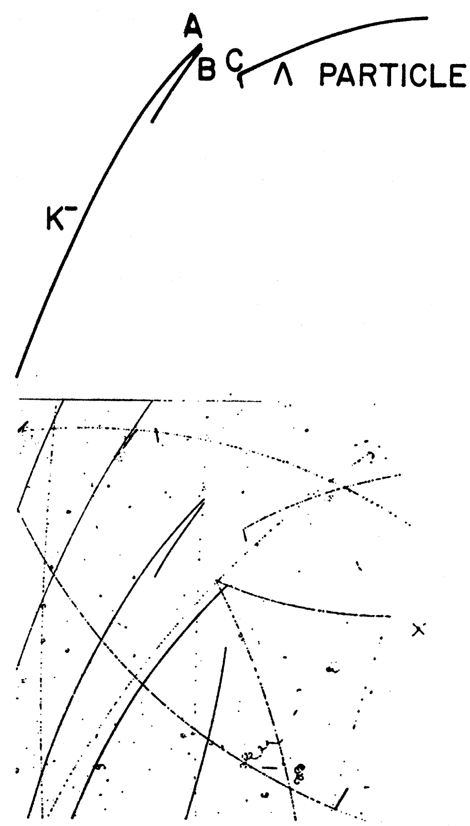

FIG. 2. A print of a portion of a frame of film containing a Λ-p elastic scattering event and a line drawing of the same event. In this event, the Λ scatters backward in the center-of-mass system, giving rise to a relatively long proton recoil.

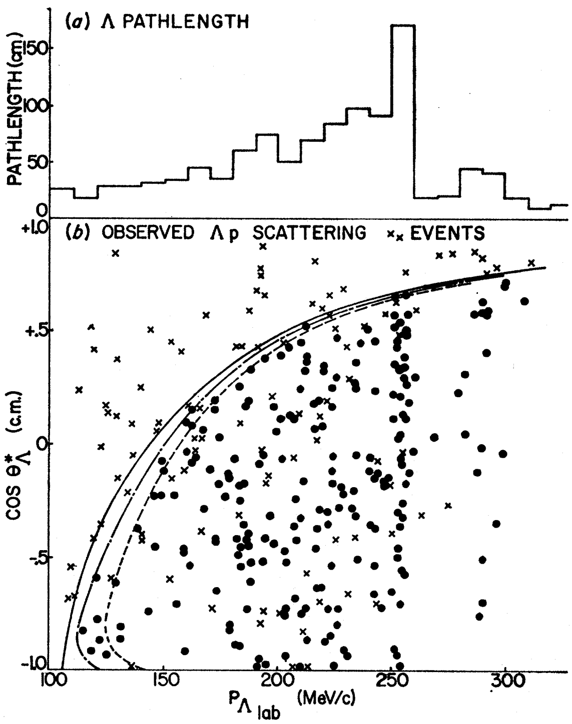

FIG. 3(a). The Λ path length as a function of the incident laboratory Λ momentum. (b) The center-of-mass scattering angle of Λ hyperons as a function of the incident Λ laboratory momentum. Λ-*p* elastic scattering events which fall below the solid curve have recoil protons whose true length is >2 mm. In addition, those events below the broken curve have weighting factors <2.5 (as discussed in the text and the Appendix.) Those events below the dashed curve have weighting factors <2.0. Λ-*p* elastic scattering events which satisfy the criteria listed in the text and have weighting factors <2.5 are indicated by dots; those events which fail one or more criteria or have weighting factors >2.5 are indicated by crosses.

event with a weighting factor larger than 2.5 was not accepted. Further details concerning the method used to determine the weighting factors are given in the Appendix. In Fig. 3(b), the 224 events which satisfy the five criteria listed above and which have weights less than 2.5 are indicated by dots; those which fail one or more of those criteria, or which have weights above 2.5, are indicated by crosses. All events with incident momenta and center-of-mass scattering angles such that they should be plotted above the solid line in Fig. 3(b) will fail criteria (iii) since such events have recoil protons of true length <2.0 mm. Thus, no event with incident Λ momentum below 110 MeV/*c* can satisfy this criterion. Only those events represented by dots (224 events) are used in the subsequent analysis. The scanning efficiency for scattering events satisfying these criteria was taken to be 98%, the measured efficiency for finding Λ's. This efficiency is consistent with and statistically more reliable than the measured efficiency for scatters.

Figure 3(a) shows the path length versus momentum distribution for a sample of 1200 Λ events. These events were randomly selected from the 95 627 Λ

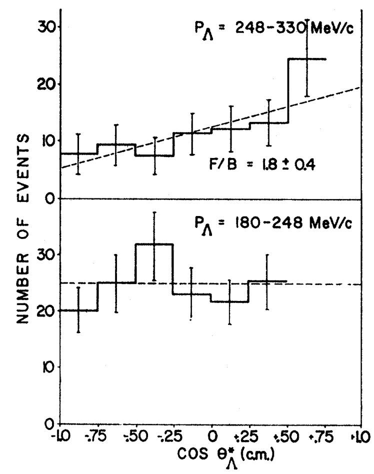

FIG. 4. The Λ-*p* elastic scattering angular distributions for different regions of Λ momentum.

decays recorded [84 527 produced in reactions (1) and (2) and 11 100 in reactions (3) and (4)] and were measured. The cutoffs (i), (ii), and (v) were applied to these events and the relevant weighting factors were used.

Figure 4 shows the angular distributions obtained for Λ-*p* scattering in two regions:

Region I: $180<p_\Lambda<248$ MeV/*c*, Λ-*p* scattering is consistent with isotropy; a forward to backward ratio of 0.9 ± 0.2.

Region II: 248 MeV/*c* $<p_\Lambda<330$ MeV/*c*, Λ-*p* scattering departs from isotropy by two standard deviations. The best-fit distribution, linear in $\cos\theta^*$, is

$$f(\theta^*)=1+(0.56\pm0.23)\cos\theta^*, \qquad (6)$$

or a forward to backward ratio $F/B=1.8\pm0.4$.

Table I lists the cross sections calculated for six different momentum intervals. The average momentum was obtained from the path length weighted as $1/k^2$ (k is the center-of-mass momentum divided by $\hbar$). The errors for each momentum interval reflect the statistical uncertainties in the number of scattering events and the number of unscattered Λ's measured for the path-length determination. In these cross-section calculations, we assumed that the scattering was isotropic in the center-of-mass up to the highest mo-

TABLE I. Cross section for Λ-*p* elastic scattering as a function of incident Λ laboratory momentum.

Momentum interval	Average momentum (MeV/*c*)	No. of accepted events	Cross section (mb)
120–150	135	14	209±58
150–180	165	28	177±38
180–210	194	49	153±27
210–240	226	54	111±18
240–270	252	59	87±13
270–330	293	20	46±11

mentum, 330 MeV/c. The cross section increases by only 5% above 250 MeV/c, if the anisotropic distribution, Eq. (6), is used. The values for the cross sections listed in Table I are in good agreement with the results of the Rehovoth-Heidelberg group.[5]

IV. ANALYSIS

The simplest phenomenological description of the s-wave Λ-p scattering assumes that the relationship

$$k\cot\delta = -1/a + \tfrac{1}{2}r_0k^2 \qquad (7)$$

holds, separately, for the singlet (total spin 0) and triplet (total spin 1) scattering. In this expression, δ is the s-wave scattering phase shift, a is the scattering length, r_0 is the effective range appropriate to the spin state involved, and k is the center-of-mass momentum divided by $\hbar$. The total s-wave cross section can then be written, in terms of the two singlet and two triplet parameters a_s, r_{0s}, a_t, and r_{0t}, as

$$\sigma = \frac{\pi}{k^2 + (-1/a_s + \frac{1}{2}r_{0s}k^2)^2} + \frac{3\pi}{k^2 + (-1/a_t + \frac{1}{2}r_{0t}k^2)^2}. \qquad (8)$$

The Λ-p elastic scattering cross-section data can then be used, together with Eq. (8), to determine the four unknown parameters.

Good fits, in the sense of χ^2, to the cross-section data in Table I, can be found for a wide variety of values of the scattering length and effective-range parameters. The set of "good" parameters is not adequately represented by a best set plus a variance matrix since there are nonlinear correlations among the variables. The set with the lowest χ^2 (2.1 for two degrees of freedom) is $a_s \simeq -2.0$ F, $r_{0s} \simeq 5.0$ F, $a_t \simeq -2.2$ F, and $r_{0t} \simeq 3.5$ F. The confidence level $P(\chi^2)$ for the best

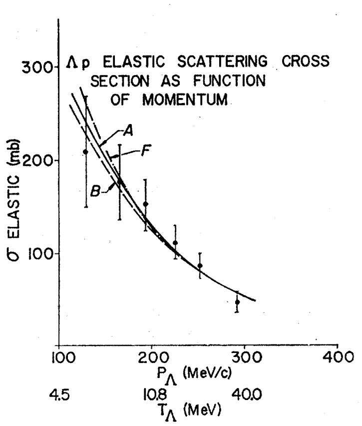

FIG. 5. The Λ-p elastic scattering cross section as a function of the incident Λ momentum. The experimental data points are plotted against the cross-section curve generated by the best-fit scattering parameters, curve A, described in the text. The dashed curves, B and F (see Table II), correspond to solutions involving pure triplet scattering and small triplet scattering. Both these cases are within one standard deviation $[(\chi^2)_{\min}+1]$ of the best-fit solution (curve A).

TABLE II. Effective-range description of Λ-p scattering.

Parameter	One-standard-deviation bound[a]	Complete solution (a_s,r_{0s},a_t,r_{0t})
a_s	$0.0>a_s>-15$ F	$B=(\ \ 0.0,\ 0.0,\ -2.4,\ 3.0)$
		$C=(-15.0,\ 11.0,\ -2.0,\ 3.0)$
r_{0s}	$0.0<r_{0s}<15$ F	$D=(\ \ 0.0,\ 0.0,\ -2.4,\ 3.0)$
		$E=(\ \ 0.0,\ 15.0,\ -2.4,\ 3.0)$
a_t	$-0.6>a_t>-3.2$ F	$F=(\ -8.0,\ 1.5,\ -0.6,\ 5.0)$
		$G=(\ -1.0,\ 3.0,\ -3.2,\ 4.5)$
r_{0t}	$2.5<r_{0t}<15$ F	$H=(\ -2.0,\ 15.0,\ -2.0,\ 2.5)$
		$I=(\ -1.0,\ 6.0,\ -0.8,\ 15.0)$

[a] Solutions were searched for in the range 0 to 15 F for r_0 and 0 to -15 F for a.

set is 0.34 which indicates that effective-range theory is a very satisfactory description of the data Λ-p scattering above 250 MeV/c is peaked forward which could indicate a p-wave interference.[12] The forward peaking also suggests that simple K^+-meson exchange forces are weak, since this would result in backward rather than forward peaking. There is no evidence for a low-energy Λ-p resonance as reported by Melissinos *et al.*[13] The recent suggestion[14] of an elastic resonance in the Λ-p system near the Σ-N threshold ($\sim$600 MeV/c) is far above the maximum momenta studied in our experiment. The Λ-p scattering cross sections as a function of momentum implied by the best set of parameters are plotted in Fig. 5 as curve A; also included in this figure are other curves and the measured cross sections for Λ-p scattering. An estimate of the one-standard-deviation extremes on the parameters, a_s, r_{0s}, a_t, and r_{0t}, has been obtained by noting the values of the parameters on the boundary $(\chi^2)_{\min}+1$ (for variations within the range 0-15 F). For the case of correlated variables, this procedure is sensitive to the effect of correlations but usually gives an extreme estimate of the one-standard-deviation limits. The bounds and associated solutions are listed in Table II. These results illustrate the range and wide variety of acceptable solutions. The singlet parameters a_s and r_{0s} are not bounded for the range of values considered, $0>a_s>-15$ F and $0<r_{0s}<15$ F. A similar procedure has been used to determine the two-standard-deviation bounds on the parameters a_s, r_{0s}, a_t, and r_{0t}, but our data do not restrict the range of solutions allowed for this case in a meaningful way. In general, our results are complicated correlated solutions in four-dimensional space which can vary within one-standard-deviation bounds from small triplet to pure triplet scattering with many acceptable intermediate solutions. To illustrate this point, Fig. 5 displays curve B (see Table II) which corresponds to pure triplet scattering and curve F which corresponds to small triplet scattering. Both

[12] B. Ram and B. W. Downs, Phys. Rev. **133**, B420 (1964).
[13] A. C. Melissinos *et al.*, Phys. Rev. Letters **14**, 604 (1965).
[14] D. Cline, R. Laumann, and J. Mapp, Phys. Rev. Letters **20**, 1452 (1968).

these cases fit the data well, within one standard deviation $[(\chi^2)_{\min}+1]$ of the best-fit solution.

The difficulty in obtaining more precise solutions from the previous analysis is due to the limited number of Λ-p scattering events.[15] In order to test this hypothesis, the assumption was made that the number of events in a future experiment could be increased by a factor to ten—a total of $\sim$2000 events. The Λ-p scattering cross-section data of Table I was used with reduced statistical errors together with the same effective-range theory analysis. The results of this trial indicate that more well-defined solutions can be found. The one-standard-deviation bounds listed in Table II for the parameters a_s, r_{0s}, a_t, and r_{0t} are reduced by a factor of $\sim$3. The most recent K^- experiments contain several million K^- mesons and therefore such studies can, in principle, be undertaken at present. Additional information, which is sensitive to scattering in the various spin states, can be obtained from a study of the scattering of polarized Λ's.[16] However, the polarized Λ hyperons are produced from in-flight K^--p and π^--p interactions and therefore are more energetic than those produced from at rest K^--p interactions. For this reason, the effective-range theory analysis may become more complicated if additional partial waves are required for the description of Λ-p scattering in this energy range.

Further analysis of current experimental results can be undertaken if theoretical assumptions are made about the form of the Λ-p interaction. This leads to the derivation of functional relationships[17,18] between a and r_0 for each spin state such as $r_{0i}=b[1-Q(s)b/a_i]$,[17] where b is the intrinsic range and $Q(s)$ depends on the potential shape chosen and the well-depth parameter s, but is almost independent of the latter. If the intrinsic range b is assumed to be the same for the singlet and triplet states, then b, a_s, or r_{0s}, and a_t or r_{0t} become the free parameters. Various assumptions can be made about the intrinsic range and/or about the shape of the Λ-p potential. In this way, the number of free parameters can be changed from four to three or to two. As an illustration, assuming a purely attractive Yukawa potential ($Q\simeq0.9$), we obtain the following one-standard-deviation bound $[(\chi^2)_{\min}+1]$ for the three parameters b, a_s, and a_t: $1.4<b<2.4$ F, $0>a_s>-9.0$ F, and $-0.8>a_t>-3.2$ F. These results do not represent a significant improvement over the bounds listed in Table II. If the range b is fixed, the number of parameters is reduced to two and the bounds are further restricted. However, there are no compelling theoretical reasons for adopting a specific value for the intrinsic range of the interaction and therefore this is not a unique method of reducing the number of free parameters required for describing Λ-p scattering. There is an extensive discussion of this procedure as applied to the analysis of Λ-p scattering data by Ali *et al.*[19] A more sophisticated theoretical model has been made by Dosch and Müller[20] to relate a_i and r_{0i}. The model of Dosch and Müller uses partial-wave amplitude dispersion theory and SU_3 invariance plus assumptions about the existence of a unitary singlet scalar meson. Relations between a and r_0 are tabulated for each spin state. The best fit to the experimental data is in good agreement with the predictions of this model.

The study of hyperfragments can yield information concerning the Λ-nucleon interaction.[1–3] The light s-shell hypernuclear systems have been studied in detail and the binding energy measurements can be expressed as volume integrals of the Λ-N potential. From the analysis of different light hyperfragments, volume integrals for the singlet and triplet interactions can be obtained. These volume integrals are related to the scattering length and effective range parameters, a_i and r_{0i}, after assuming a specific value for the intrinsic range b. The hyperfragment analysis, therefore, depends on fundamental theoretical assumptions concerning the form of the Λ-N interaction. However, the situation is considerably more involved since there are many underlying complications present in the hyperfragment analysis. Bodmer[21] has suggested that information derived from the study of $_{\Lambda}He^3$ may not be directly applicable to Λ-N scattering since the large triplet interaction may be substantially underestimated. In general, because of the tight binding and saturation of the nuclear forces in He^4, it is expected that the structure of $_{\Lambda}He^5$ might not reliably reflect the two-body forces involved in scattering. The lighter hyperfragments are, however, more loosely bound and two-body interactions should dominate their properties. But for these systems, there are still possible complications from the presence of spin-flip transitions and charge-symmetry breaking effects of the Λ-N interaction. Some of the predictions for a_s and a_t from the study of hyperfragment systems do not agree well with the more direct Λ-p scattering results. However, recently Herndon and Tang[22] have obtained good agreement between hyperfragment calculations and Λ-p scattering results by assuming larger values for the intrinsic range (>1.5 F).

V. CONCLUSIONS

From the analysis of this bubble chamber experiment, we deduce that low-momentum Λ-p elastic scattering

[15] An extension of Λ-p scattering cross section to lower incident Λ momentum would narrow the range of allowed solutions. Because of the short proton recoils associated with such events, this extension seems beyond the scope of present experimental techniques.

[16] C. Gardiner and T. Welton, Phys. Rev. Letters 3, 281 (1959).

[17] J. J. deSwart and C. Dullemond, Ann. Phys. (N. Y.) **19**, 458 (1962).

[18] R. D. Levee and R. H. Pexton, Nucl. Phys. **55**, 34 (1964).

[19] S. Ali, M. E. Grypeos, and L. P. Kok, Phys. Letters **24B**, 543 (1967).

[20] H. G. Dosch and V. F. Müller, Phys. Letters **19**, 320 (1965).

[21] A. Bodmer, Phys. Rev. **141**, 1387 (1966).

[22] R. C. Herndon and Y. C. Tang, Phys. Rev. **159**, 853 (1967).

is satisfactorily described by the s-wave effective-range approximation involving two singlet and two triplet parameters a_s, r_{0s}, a_t, and r_{0t}. Λ-p scattering above 250 MeV/c is peaked forward which could indicate a p-wave interference. However, the main conclusion of our study is that the effective-range analysis results in complicated correlated solutions in four-dimensional space which can vary within one-standard-deviation bounds from small triplet to pure triplet scattering with many acceptable solutions. Any further deductions from this experiment depend strongly on the nature of the particular theoretical assumptions introduced.

ACKNOWLEDGMENTS

We wish to thank the University of Maryland scanning and measuring staff for their diligent efforts. The assistance of Professor H. Courant, Professor H. Filthuth, Dr. A. Segar, and Professor W. Willis in early aspects of this experiment is acknowledged. The contributions of Professor T. B. Day and Professor R. G. Glasser in all phases of this work were important. Finally, we appreciate the valuable discussions with Professor G. A. Snow.

APPENDIX: DETERMINATION OF WEIGHTS FOR (Λ-p) SCATTERING EVENTS

A set of geometric criterion were applied to the Λ-proton scattering events:

(i) The point of origin of the Λ was required to be within a specified fiducial volume.

(ii) The projected length of the incident Λ was required to be greater than 0.5 mm.

(iii) The projected length of the recoil proton was required to be greater than 2.0 mm.

(iv) The projected length of the scattered Λ was required to be greater than 0.5 mm.

(v) The projected length of the proton from the Λ decay was required to be greater than 1.0 mm.

The criteria (i) and (ii) were also applied to the direct Λ's used to determine the path-length distribution. The application of these criteria do not, therefore, affect the measured cross sections in a systematic way. Criteria (iii)–(v) are applied only to the scattering events and to provide an unbiased cross section, it is necessary to correct the number of acceptable events. The procedure employed was to calculate a weight for each event corresponding to the inverse of the probability that an event with the observed incident momentum and scattering angle would satisfy criteria (iii)–(v).

This probability was determined by a systematic sampling of the universe of possible events with a given incident momentum $P_{\rm in}$ and center-of-mass scattering angle, θ^*. $P_{\rm in}$ and $\cos\theta^*$ are the coordinates of the scatter plot, Fig. 3. Events were simulated on a computer in the following manner:

(a) A Λ of momenta $p_{\rm in}$ was produced with dip α.

(b) This Λ was scattered off a target proton with scattering angle θ^* and azimuth ψ^* ($\psi^*=0$ corresponds to a scattering in vertical plane).

(c) The projected length of the scattered proton in the laboratory was determined.

(d) The scattered Λ was made to decay with the center-of-mass angle of the proton being β and its azimuth Φ ($\Phi=0$ corresponding to a decay in vertical plane).

(e) The projected length of the decay proton in the laboratory was determined.

For each set of the parameters $P_{\rm in}$ and $\cos\theta^*$, 80 000 simulated events were generated with 10 values of $\sin\alpha$ uniformly spaced from 0 to 1; 20 values of ψ^* from 0 to π; 20 values of $\cos\beta$ from -1 to 1, and 20 values of Φ from 0 to π. For each simulated event an associated acceptance probability was determined:

$$f_i=l_1l_2g\,,$$

where $l_1(l_2)=0$ or 1 as the projected length of the recoil (decay) proton is less than or greater than the cutoff given in criterion (iii) [(iv)], and $g=\exp[-\lambda M_\Lambda/(P'\cos\alpha'\,C\tau_\Lambda)]$ is the probability that a Λ of momenta P' and dip α' after the scatter will have projected length greater than λ, the cutoff specified in criterion (iv). The weight associated with the measured scattering event is

$$\omega(P_{\rm in},\cos\theta^*)=1/\bar{f}\,,$$

where $\bar{f}$ is the average of the individual f_i over the 80 000 simulated events.

This procedure explicitly assumes isotropic production and decay of the Λ and azimuthal isotropy of the scattering. The weighting corrects for loss of events in the region of $P_{\rm in}$ and $\cos\theta^*$ for which acceptable events are physically allowed. Above the solid curve on the diplot, Fig. 3, all proton recoils have true length less than 2.0 mm, the cutoff used in criterion (iv). Further, the probability of an event being accepted rises very rapidly from zero below that line. To avoid weights which are large and subject to significant experimental error, a sixth criterion was introduced:

(vi) The weight associated with an event which satisfies the above criteria must be less than 2.5.

As this weight is a function of $P_{\rm in}$ and $\cos\theta^*$ only, contours of equal weight can be drawn on the diplot. The contour for weight 2.5 is shown as the broken curve and, for comparison, the contour for weight 2.0 is shown as a dashed curve. All events below and to the right of the broken curve have weights below 2.5 and hence satisfy criterion (vi). Determination of the total cross section was made by compensating for loss of events outside this curve on the basis of an assumption about the scattering distributions which are described in the text.